# Accurate Characterization of T/R Modules with Consideration of Amplitude/Phase Cross Effect in AESA Antenna Unit

Chang-Soo Ahn, Sang-Mi Chon, Seon-Joo Kim, Young-Sik Kim, and Juseop Lee

In this paper, an accurate characterization of a fabricated X-band transmit/receive module is described with the process of generating control data to correct amplitude and phase deviations in an active electronically scanned array antenna unit. In the characterization, quantization errors (from both a digitally controlled attenuator and a phase shifter) are considered using not theoretical values (due to discrete sets of amplitude and phase states) but measured values (of which implementation errors are a part). By using the presented procedure for the characterization, each initial control bit of both the attenuator and the phase shifter is closest to the required value for each array element position. In addition, each compensated control bit for the parasitic cross effect between amplitude and phase control is decided using the same procedure. Reduction of the peak sidelobe level of an array antenna is presented as an example to validate the proposed procedure.

Keywords: AESA antenna, T/R module, characterization, multi-function chip.

## I. Introduction

Active electronically scanned array (AESA) radars with transmit/receive (T/R) modules have been studied and developed for decades because they provide enhanced system functionality and performance compared to mechanically scanned array (MSA) radars [1]–[3].

An AESA radar implements rapid beam steering by independently setting the phase of each T/R module's phase shifter (each T/R module is connected to an array element), whereas an MSA radar is limited to beam steering by using hydraulically or electrically controlled gimbal to physically move the array for search.

In addition, an AESA radar can control the shape of an antenna beam by adjusting the amplitude of attenuators in T/R modules connected to each array element [4]. Thus, an AESA radar has improved search and track performance because of beam agility [5].

Figure 1 shows the configuration of an AESA antenna unit in a radar system [6]–[8]. Radar systems usually have a separate receive beamformer for each monopulse beam for angle tracking of targets, such as sum ($\Sigma$), azimuth difference ($\Delta$Az), and elevation difference ($\Delta$El). In addition, a guard channel is applied to blank sidelobe detection. The AESA antenna unit consists of radiating elements and an antenna structure; T/R modules and associated control circuitry; RF beamformers; DC power distribution; and a beam steering controller.

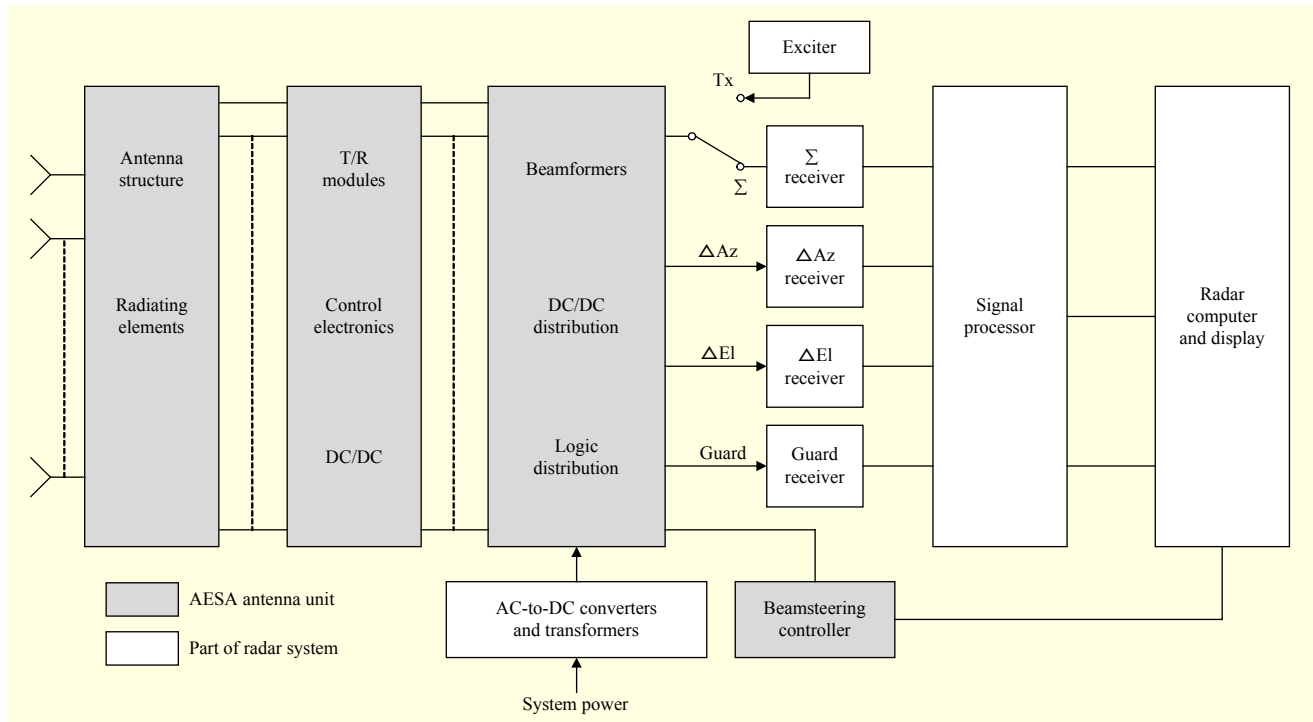Because there are usually hundreds or thousands of radiators

Fig. 1. Configuration of AESA antenna unit in radar system.

and T/R modules, and a lot of networks connecting them, in an AESA antenna unit, considerable amplitude and phase differences among the paths from each array element to each receive beamformer output are produced; these differences can cause degradation of radiation performance.

In general, degradation of radiation performance of an AESA antenna unit occurs due to the quantization of both amplitude taper and phase shift at each array element [9].

Several methods have been proposed to enhance antenna gain and achieve more precise beam pointing and broader null forming [10]–[12].

In this paper, an accurate characterization of a fabricated X-band T/R module with a multi-function chip is presented to improve the radiation performance of an AESA antenna unit.

The process through which to generate control data that is to be read by the multi-function chip is described through several steps. In particular, we describe the procedure to derive each initial control bit of both the attenuator and the phase shifter, taking into consideration the implementation errors of the T/R module. It is also shown that each control bit for the compensation of the parasitic cross effect between amplitude and phase control of the T/R module can be derived using the same procedure.

A 16 by 16 planar array antenna unit with T/R modules is considered to verify the proposed procedure. It is shown that the proposed procedure can reduce the peak sidelobe level of the array antenna unit.

## II. Generation of Control Data in AESA Antenna Unit

An AESA antenna unit should generate and calculate control data in T/R modules responding to beam-control parameters for specified beam shapes and directions [13]. The generation of control data in an AESA antenna unit can be described as shown in Fig. 2.

In the first step, a set of *desired settings* (without any imperfections) for the array elements is generated from an "Antenna generator" function. The set of desired settings depends on several factors, such as main beam direction $(u, v)$, center frequency, taper information for beam shape, antenna map, and active element pattern, as indicated in Fig. 2.

An antenna map features a set of vectors — one for each array element that commences in the array antenna phase center and ends in the element phase center. The "active element pattern" function describes the radiation pattern for each array element, when placed in the array surrounded by all neighboring elements [14].

The parameters $u$ and $v$ indicate the direction of a beam within a sine-space coordinate system. Sine space is a hemispherical projection of three-dimensional space onto a plane of an array [9].

In the second step, a calibration value stored in the "Antenna Correction" function is subtracted from the set of desired settings. This subtraction results in a new set of desired settings, which we call "corrected desired settings."
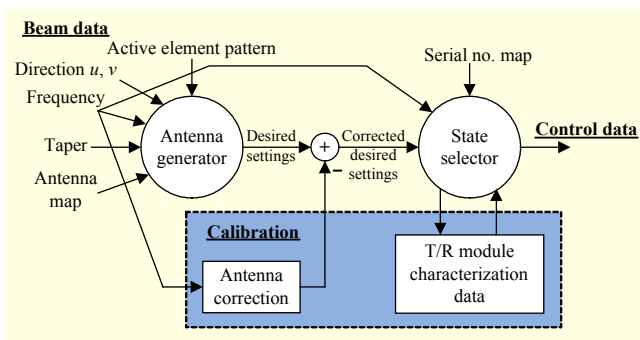
Fig. 2. Generation of control data and usage of calibration data in AESA antenna unit.



Fig. 3. Hardware components, and placement of data and calculations.

Table 1. Error sources of amplitude and phase deviation in AESA array unit.

| Error source | Error type |
|---|---|
| T/R modules | Non-linear |
| Difference between T/R modules and networks for dividing and combining | Linear |
| Difference for beamformers | Linear |
| Manufacturing tolerance of radiating elements spacing | Linear |
| Difference by connection between T/R modules and radiating elements | Linear |



Fig. 4. Block diagram of T/R module.

An antenna correction table containing phase and amplitude correction values for each frequency is constructed. The correction values are amassed on a near-field antenna test range using a method known as single element adjustment [15], [16].

Table 1 shows the error sources of the amplitude and phase differences among the paths from each array element to each receive beamformer output. All error sources except for "T/R modules" are linear and can finally be corrected through a near-field antenna test. The error by "T/R modules" is nonlinear; thus, the characterization described in Section III is necessary.

Prior to the commencement of data collection for the antenna correction table, it is required that the T/R module characterization data is updated with the latest available data for all currently installed T/R modules. In the last step, the corrected desired settings are converted to control data. This conversion is preferably executed in each T/R module as it is dependent normally on both the temperatures and the serial numbers of the T/R modules. The temperature of each T/R module can be measured internally, and a T/R module's serial number should preferably be stored within its own non-volatile memories to facilitate the replacement of T/R modules without the need, for example, to update an externally stored database. Figure 3 shows how data and calculations can be placed in the different components.
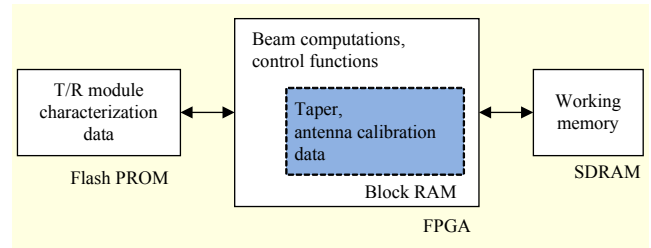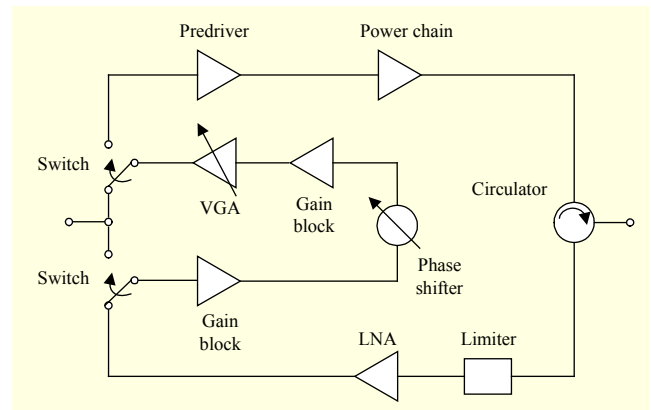
## III. Characterization of T/R Modules

Since a T/R module is a key component of an AESA radar (from the perspective of cost), related fields have reached maturity through huge academic and industrial investment [17].

Figure 4 shows a block diagram of a typical common-leg T/R module [18]. Recently, Monolithic Microwave Integrated Circuit (MMIC) chips having several functions such as signal amplifying, controlling, and T/R switching have been investigated as a single-core chip [19]–[21].

In this section, an accurate characterization of a fabricated X-band T/R module with a multi-function chip is presented for the generation of control data in an AESA antenna unit.

### 1. Method

A fabricated X-band T/R module with a multi-function chip is shown in Fig. 5. The lid is removed partially to show the MMIC chips. A hetero-junction multilayer substrate with one FR4 substrate for digital signals and three ceramic substrates (12 mil RO4003) for RF signals is used for low cost, and a dual-pack architecture is selected to reduce the size and weight of the T/R module. The multi-function chip is an OMMIC CGY2170XUH, which contains a phase shifter, an attenuator, and switches. The control values of both the attenuator and the phase shifter are summarized in Table 2. There are
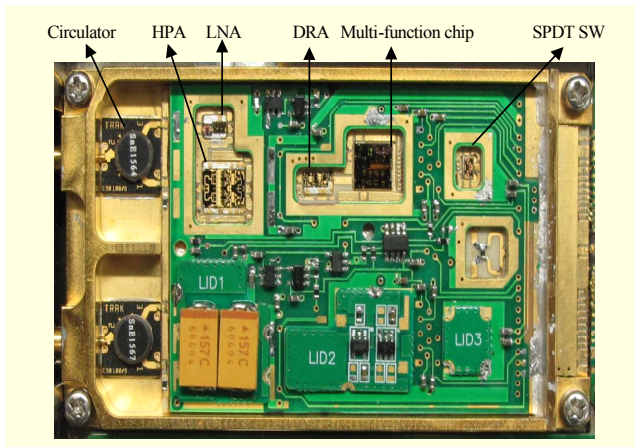
Fig. 5. Fabricated X-band T/R module with multi-function chip.

Table 2. Control values of attenuation and phase shifter at 10 GHz.

| Control bit order, $i$ ($N = 6$) | | 1 | 2 | 3 | 4 | 5 | 6 |
|---|---|---|---|---|---|---|---|
| Attenuator | Target value (dB) | 0.50 | 1.00 | 2.00 | 4.00 | 8.00 | 16.00 |
| | Measured value (dB) | 0.50 | 0.95 | 2.00 | 4.00 | 7.80 | 15.40 |
| | Phase change (°) | 0.16 | 1.77 | 0.20 | –3.80 | –3.26 | –3.60 |
| Phase shifter | Target value (°) | 5.60 | 11.20 | 22.50 | 45.00 | 90.00 | 180.00 |
| | Measured value (°) | 5.55 | 13.00 | 22.70 | 42.30 | 86.00 | 183.00 |
| | Amplitude change (dB) | –0.29 | –0.38 | –0.11 | –0.63 | –1.11 | –0.94 |

discrepancies between the measured and the quantized target values due to implementation errors. In addition, the parasitic cross-effect between amplitude and phase controls is depicted. In other words, the attenuator is intended to change amplitude, but its phase also changes during the process of attenuation control. On the other hand, the phase shifter is intended to change phase, but its amplitude also changes during the process of phase-shift control. The phase shifter is intended to adjust the phase in a signal path, but it produces parasitic amplitude change at the time of controlling it. Table 2 shows this parasitic amplitude change for each bit of each initial control bit in the digital phase shifter. Hence, the total parasitic amplitude change depends on which bits are in use at the time of controlling the phase shifter. The topologies used for implementing each bit in Table 2 are different from one another, which leads to non-monotonic variation in parasitic amplitude change with increasing bit number. Thus, these measured values including the cross effect should be taken into

consideration to find the final control bits matched to the required values of amplitude taper and phase shift for each array element. Practically, the values can be changed with operating conditions such as frequency, temperature, different implementation errors of each T/R module, and so on. However, the values in Table 2 are used for demonstration purposes in this paper; this alone is sufficient to demonstrate the usage of the proposed procedure in the case of other possible values.

The basic procedure of the characterization for amplitude and phase in a T/R module is shown in Fig. 6. First, the initial control bits for each array element, for the nearest quantized values with implementation errors to the required values, can be obtained through the proposed procedure. To this end, measured values in Table 2 are used for $Q_i$ (the controlled value corresponding to the $i$th bit). For example, if the required amplitude taper value for a certain array position is –24.64 dB, then the initial control bit will be determined as 110011; that is, –24.65 dB through the proposed procedure. The initial control bits for all array elements for the phase shifter are obtained in the same manner. The discrepancy between the required and represented values by the initial control bits for all array elements will be no more than the half of the quantized value corresponding to the least significant bit.

Second, the control bits matched to the amplitude change by each phase-shifter state can be derived by using the same flow chart as in Fig. 6, except for the fact that $X$ would instead represent the total amplitude change value with regard to each phase-shifter state. For example, the total amplitude change by a phase-shifter state of 111000 is –0.78 dB (from Table 2) and the corresponding attenuator control bit will be determined to be 010000; that is, –0.95 dB. Thus, we will obtain the attenuator control bits matched to the amplitude change at all 64 phase-shifter states and store them to the memory in the T/R module. Then, their *callback* will be performed easily when the phase shifters of the T/R modules at each element for beam steering in a certain direction are set to the initial control bits, as depicted in Fig. 7. The corresponding phase-shifter control bits for the phase change by each attenuator state can be obtained in the same manner. The computational load for each new pointing control in real-time systems can be minimized because a trans coding table is pre-calculated and stored within the memory of each T/R module.

## 2. Verification

To verify the proposed method, an array antenna is considered — the details of which are given in Table 3. To characterize only T/R modules, we assume that all array elements have an isotropic radiation pattern and that the mutual
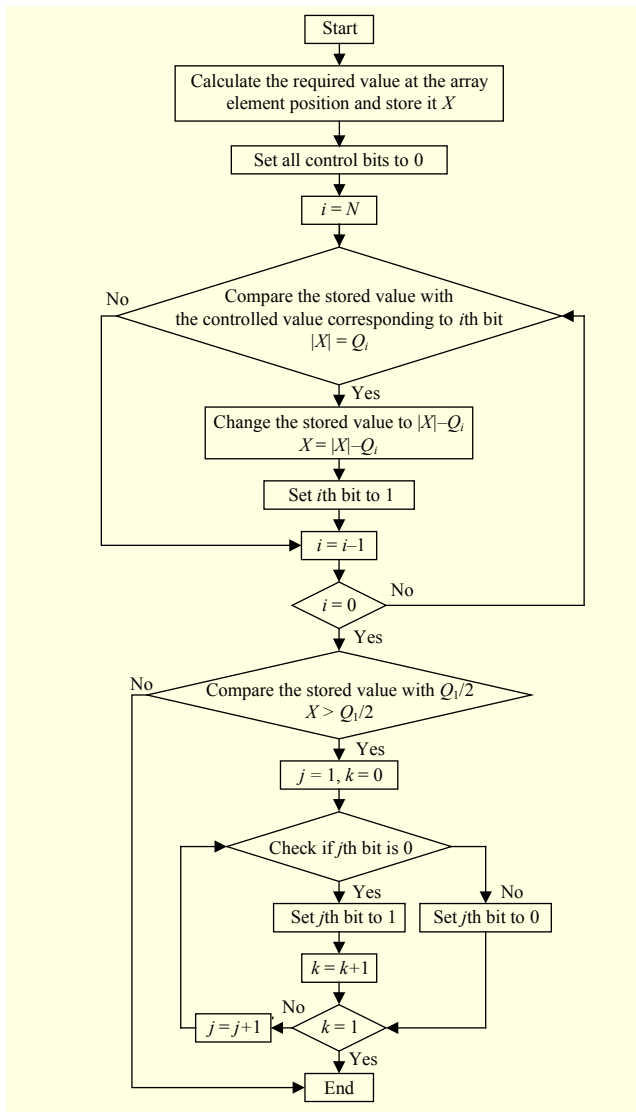
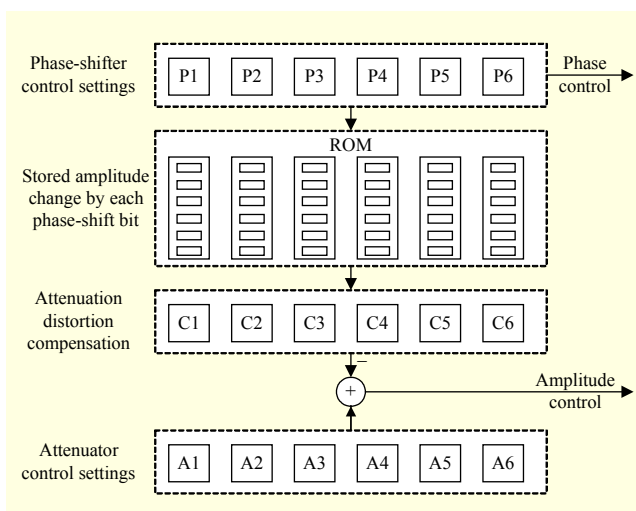Fig. 6. Basic procedure for characterization of T/R module.



Fig. 7. Compensation of amplitude change by phase shifter.

Table 3. Parameters of AESA antenna unit in analysis.

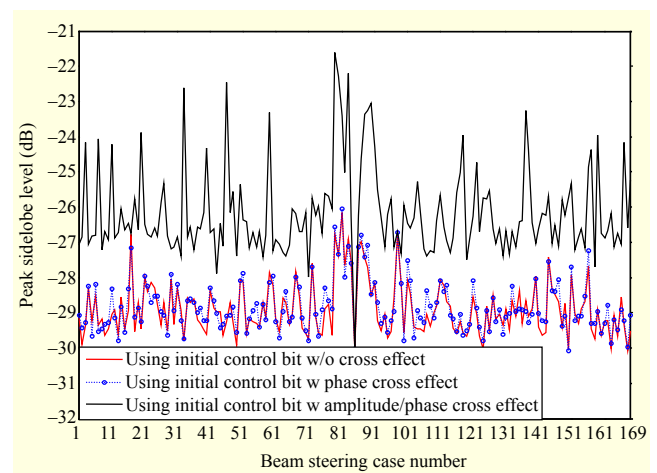| Parameter | Value |
|---|---|
| Type | Planar array |
| Number of elements | $16 \times 16$ |
| Element grid | Triangular grid |
| Element spacing | $dx = 19.5$ mm, $dy = 14.7$ mm |
| Amplitude weighting | −30 dB Taylor distribution, $\bar{n} = 5$ |



Fig. 8. Peak sidelobe levels of array antenna for number of beam steering cases under assumption that T/R modules are operated using initial control bits without cross effect, with phase cross effect, and with amplitude/phase cross effect, respectively.

coupling between them is neglected.

Peak sidelobe levels of the array antenna for a number of beam steering cases are shown in Fig. 8, where T/R modules are operated using initial control bits. The beam steering cases in Fig. 8 represent that the array antenna steers a beam in an orderly manner in 5° increments from −30° to +30° in both azimuth and elevation angles. In other words, the beam steering case numbers #1 and #2 represent that the array antenna is directed to (−30°, −30°) and (−25°, −30°) in azimuth and elevation angles, respectively. Thus, the beam steering case numbers #85 and #169 represent that the array antenna steers the beam at (0°, 0°) and (+30°, +30°) in azimuth and elevation angles, respectively.

The thin solid line in Fig. 8 shows the peak sidelobe level when initial control bits for a −30 dB peak sidelobe level are used under the assumption that there is no cross effect. The peak sidelobe level is higher than the desired value due to both the quantization and implementation errors. The maximum peak sidelobe level in this case is −26.15 dB at beam steering case #81; that is, (−20°, 0°) direction.

Table 4. Values obtained from procedure for compensated control bit of attenuator at first array element.

| Parameter | Value |
|---|---|
| Required attenuation | 26.74 dB |
| Initial control bits for the attenuator (A) | 111011 |
| Measured attenuation with A | 26.65 dB |
| Required phase shift | 243.00° |
| Initial control bits for the phase shifter (B) | 110101 |
| Measured phase shift with B | 243.85° |
| Amplitude change with B (C) | −2.24 dB |
| Control bit matched to C | 001000 |
| Compensated control bits for the attenuator (D) | 110011 |
| Measured attenuation with D | 24.65 dB |
| Resultant attenuation (C + D) | 26.89 dB |
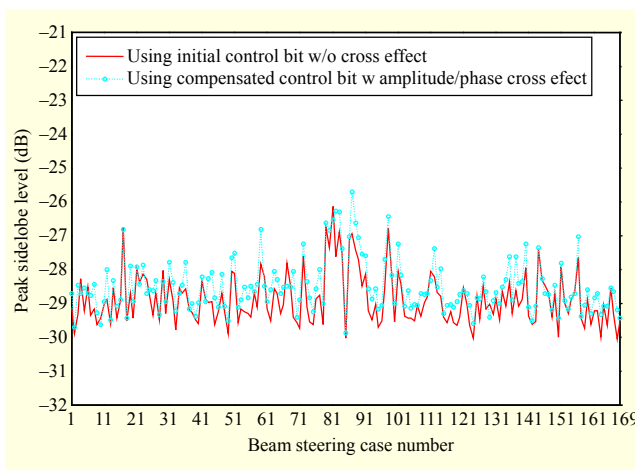


Fig. 9. Peak sidelobe levels of array antenna for number of beam steering cases, under assumption that T/R modules are operated using initial control bits without cross effect and compensated control bits with amplitude/phase cross effect, respectively.

The dotted line in Fig. 8 shows the peak sidelobe level when the cross effect of the attenuator comes into play. The additional phase change by the initial control bits of the attenuators for each array element are added to the phase by the initial control bits of the phase shifters. It shows there is little difference from the first case.

The thick solid line in Fig. 8 shows the peak sidelobe level when both the cross effect of the attenuator and the cross effect of the phase shifter accur. The peak sidelobe level in this case is largely degraded, and the array antenna has a maximum peak sidelobe level of −21.6 dB in the case of beam steering case #79; that is, (−30°, 0°) direction. The peak sidelobe level with

cross effect of the phase shifter is not shown for the sake of clarity within the figure; it is similar to the third case.

Thus, compensation of amplitude change through control of the phase shifter is only required for improvement of the peak sidelobe level. The compensated control bits can be obtained by subtracting the control bits matched to the amplitude change by each phase-shifter state (as described in Section III) from the initial control bits for the attenuators. Table 4 shows the values obtained from the procedure for the compensated control bit of the attenuator at the first array element when the beam of the antenna unit in Table 3 is directed to (−30°, −30°), for example. It is verified that the resultant attenuation of the T/R module at the array element is close to the required value from the theoretical calculation through the procedure.

The dotted line in Fig. 9 shows the peak sidelobe level when compensated control bits (to reduce the cross effect of the phase shifter) are used, under the assumption that both types of cross effect are in existence. The peak sidelobe level in this case is similar to the first case in Fig. 8. The maximum peak sidelobe level is −25.71 dB in the case of beam steering case #87; that is, (+10°, 0°) direction.

Obviously, the compensated control bits of the attenuators cause the additional phase changes. However, the related beam pointing error is negligible when a 6-bit phase shifter is utilized in the antenna unit (comprising 256 elements) [8], [22]–[24].

## IV. Conclusion

The generation process of control data for *corrected settings* of the amplitude and phase in an AESA antenna unit is described for desired and accurate beam shaping and steering. In particular, an accurate, practical characterization using data from a fabricated X-band T/R module with a multi-function chip is presented — the likes of which is invaluable to engineers who are working on calibrations of AESA antennas. Each initial control bit of both the attenuator and the phase shifter is derived through the proposed procedure. It represents the realizable and closest value to the desired amplitude and phase for each array element. In addition, each compensated control bit for the parasitic cross-effect between amplitude and phase control is decided in the same manner. Reduction of the peak sidelobe level of an array antenna using the compensated control bit is verified.

## References

[1] A. Farina et al., "AESA Radar-Pan-Domain Multi-function Capabilities for Future Systems," *IEEE Int. Symp. Phased Array Syst. Technol.*, Waltham, MA, USA, Oct. 15–18, 2013, pp. 4–11.

[2] P. Sgambato et al., "System Manager for AESA Radar Systems," *IEEE Radar Conf.*, Arlington, VA, USA, May 10–15, 2015, pp. 1734–1738.

[3] R. Bil and W. Holpp, "Naval Radar Trends: a Look Back-a Look Forward," *Int. Radar Symp.*, Dresden, Germany, June 24–26, 2015, pp. 13–19.

[4] E.R. Billam, "MESAR-the Application of Modern Technology to Phased Array Radar," presented at *the IEE Tutorial Meeting Phased Array Radar*, London, UK, Sept. 18, 1989, pp. 5/1–5/16.

[5] R. Hendrix, "Aerospace System Improvements Enabled by Modern Phased Array Radar-2008," *IEEE Int. Radar Conf.*, Rome, Italy, May 26–30, 2008, pp. 1–6.

[6] A.K. Agrawal et al., "Active Phased Array Antenna Development for Modern Shipboard Radar System," *Johns Hopkins APL Tech. Dig.*, vol. 22, no. 4, 2001, pp. 600–613.

[7] A.K. Agrawal and E.L. Holzman, "Beamformer Architectures for Active Phased-Array Radar Antennas," *IEEE Trans. Antennas Propag.*, vol. 47, no. 3, Mar. 1999, pp. 432–442.

[8] M. Skolnik, "*Introduction to Radar Systems*," 3rd ed., New York, NY, USA: McGraw-Hill, 2001.

[9] A.D. Brown, "*Electroncially Scanned Arrays MATLAB Modeling and Simulation*," Boca Raton, FL, USA: CRC Press, 2012.

[10] S.H. Son, W. Hwang, and S.I. Jeon, "Gain Enhancement of Large Phased Array Antennas by Phase Error Correction," *IEEE Antennas Propag. Soc. Int. Symp.*, Honolulu, HI, USA, June 9–15, 2007, pp. 137–140.

[11] W. Jiang et al., "Comparison of Random Phasing Methods for Reducing Beam Pointing Errors in Phased Array," *IEEE Trans. Antennas Propag.*, vol. 51, no. 4, Apr. 2003, pp. 782–787.

[12] N. Nakamoto et al., "Phase Optimization for Accurate Beam Forming of Phased Array with Element Field Errors at Every Phase Shift," *IEEE Int. Symp. Phased Array Syst. Technol.*, Waltham, MA, USA, Oct. 15–18, 2013, pp. 693–697.

[13] P.N. Drackner and B. Engstrom, "An Active Antenna Demonstrator for Future AESA-Systems," *IEEE Int. Radar Conf.*, Arlington, VA, USA, May 9–12, 2005, pp. 226–231.

[14] D.M. Pozar, "The Active Element Pattern," *IEEE Trans. Antennas Propag.*, vol. 42, no. 8, Aug. 1994, pp. 1176–1178.

[15] S. Moore et al., "AMSAR Active Phased Array Antenna," *IET Int. Conf. Radar Syst.*, Edinburgh, UK, Oct. 15–18, 2007, pp. 1–4.

[16] I. Seker, "Calibration Methods for Phased Array Radars," *Proc. SPIE*, vol. 8714, May 2013, pp. 1–15.

[17] M. Pirkl and W. Holpp, "From Research to Application: How Phased Array Radars Conquered the Real World," *Int. Radar Symp.*, Dresden, Germany, June 19–21, 2013, pp. 17–21.

[18] A. Agrawal, R. Clark, and J. Komiak, "T/R Module Architecture Tradeoffs for Phased Array Antennas," *IEEE MTT-S Int. Microw. Symp. Dig.*, San Francisco, CA, USA, June 17–21, 1996, pp. 995–998.

[19] W. Ciccognani et al., "A Compact High Performance X-Band Core-Chip with on Board Serial-to-Parallel Conversion," *European Mircrowave Conf.*, Paris, France, Sept. 28–30, 2010, pp. 902–905.

[20] J.-C. Jeong et al., "An S-Band Multifunction Chip with a Simple Interface for Active Phased Array Base Station Antennas," *ETRI J.*, vol. 35, no. 3, June 2013, pp. 378–385.

[21] T. Dinc et al., "X-Band SiGe Bi-Complementary Metal-Oxide Semiconductor Transmit/Receive Module Core Chip for Phased Array Radar Applications," *IET Microw., Antennas Propag.*, vol. 9, no. 9, June 2015, pp. 948–956.

[22] C.J. Miller, "Minimizing the Effects of Phase Quantization in an Electronically Scanned Array," *Proc. Symp. Electronically Scanned Array Techn. Appl.*, Rome, NY, USA, July 1964, pp. 17–38.

[23] R.J. Mailloux, "*Phased Array Antenna Handbook*," 2nd ed., Norwood, MA, USA: Artech House, 2005.

[24] K.R. Carver, W. Cooper, and W. Stutzman, "Beam Pointing Errors of Planar Phased Arrays," *IEEE Trans. Antennas Propag.*, vol. 21, no.2, Mar. 1973, pp. 199–202.

**Chang-Soo Ahn** received his BS and MS degrees in electrical engineering from Korea University, Seoul, Rep. of Korea, in 2002 and 2005, respectively, and is currently working toward his PhD degree at Korea University. In 2005, he joined the Agency for Defense Development, Daejeon, Rep. of Korea, where he is currently a senior researcher. His research interests include airborne AESA radar system design and analysis, operational modes design, and radar resource management.

**Sang-Mi Chon** received her PhD degree in electrical engineering from Pohang University of Science and Technology, Rep. of Korea, in 2006. In 2006, she joined LIGNEX1, Yongin, Rep. of Korea, where she is currently a chief research engineer. Her research interests include active array antenna design and AESA radar system development.

**Seon-Joo Kim** received his BS and MS degrees in electrical engineering from Aju University, Suwon, Rep. of Korea, in 1986 and 1988, respectively. In 1988, he joined the Agency for Defense Development, Daejeon, Rep. of Korea, where he is currently a principal researcher. His research interests include airborne AESA radar development and core technologies research.

**Young-Sik Kim** received his BS degree in electronics engineering from Korea University, Seoul, Rep. of Korea, in 1973 and his MS and PhD degrees in electrical engineering from the University of Massachusetts at Amherst, MA, USA, in 1986 and 1988, respectively. From 1988 to 1989, he was a post doctoral research fellow at the University of Massachusetts at Amherst. From 1988 to 1993, he was with the Mobile Communications Division, Korea Electronics and Telecommunications Research Institute, Daejeon, Rep. of Korea. In 1993, he joined Korea University, where he is currently a professor. His research interests include millimeter-wave antennas and front-end systems and mobile telecommunication systems.

**Juseop Lee** received his BS and MS degrees in radio science and engineering from Korea University, Seoul, Rep. of Korea, in 1997 and 1999, respectively, and his PhD degree in electrical engineering from the University of Michigan, Ann Arbor, USA, in 2009. In 2001, he joined ETRI, Daejeon, Rep. of Korea, where he was involved in the design of passive microwave equipment for Ku- and Ka-band communications satellites. In 2005, he joined the University of Michigan, where he was a research assistant and graduate student instructor with the Radiation Laboratory, and where his research activities focused on millimeter-wave radars and synthesis techniques for multiple-passband microwave filters. In 2009, he joined Purdue University, West Lafayette, IN, USA, where he was a postdoctoral research associate, and where his activities included the design of adaptable RF systems. In 2012, he joined Korea University, where he is currently an associate professor. His research interests include RF and microwave components, satellite transponders, wireless power transfer, and electromagnetic theories. He was a recipient of the Graduate Fellowship presented by the Korea Science and Engineering Foundation, Daejeon, Rep. of Korea and the Rackham Predoctoral Fellowship presented by the Rackham Graduate School, University of Michigan. He was also the recipient of the IEEE Microwave Theory and Techniques Society Graduate Fellowship.